Appl. Phys. A (2016)122:524
DOI 10.1007/s00339-016-0056-1

Applied Physics A
Materials Science & Processing

Nanoparticle-based concretes for the restoration of historical and contemporary buildings: a new way for CO_2 reduction in architecture

Enrico Greco[1] · Enrico Ciliberto[1] · Pietro Damiano Verdura[1] · Elio Lo Giudice[2] · Giuseppe Navarra[2]

Received: 1 August 2015 / Accepted: 15 April 2016

Abstract The production of the cement is a highly energy-intensive process and contributes to the release of pollutants into the atmosphere due to both the chemical reactions occurring in the kiln and, in most cases, the burning of fossil fuels for power production. So, the reduction of the cement content in a concrete would be indirectly useful to decrease the pollutant emissions in the atmosphere. The results of our investigation indicate that the replacement levels of cement by the 4 % of nanoparticles show a positive increasing of many physical and chemical properties allowing a relevant saving of cement content inside a concrete mixture. The compressive strengths, tensile splitting, propagations of ultrasonic pulses and water permeability tests were investigated on different models and realistic structures by the ISO EN rules. The influence of the nanoparticles on physical and mechanical properties was measured at different ripening times. Both silica and iron oxides make cement pastes harder and accelerated hydration processes of the cements. A remarkable decreasing in water permeability was also observed showing that nanoconcretes can be used as innovative restoration systems for cement-based historical and contemporary artefacts in order to avoid carbonation processes. Moreover, a smaller quantity of cement binder inside the mortar causes relevant positive effects on the reduction of carbon dioxide emission in the atmosphere.

✉ Enrico Greco
egreco@unict.it

[1] Università degli Studi di Catania, Viale A. Doria 6, 95125 Catania, CT, Italy

[2] DISMAT srl, c.da Andolina SS 122, km 28, 92024 Canicattì, AG, Italy

1 Introduction

Concrete, undoubtedly, is known as one of the most useful materials around the world, and it has been used worldwide for both the construction of historical buildings (from nineteenth century) and contemporary buildings of ordinary and extraordinary importance.

The buildings of modern architecture, of recognized value, must be fully preserved in all their parts. Both the technicians and theorists of the restoration are being more unanimously agreed that the works of contemporary architects must be protected for their values of uniqueness, formal content and educational values.

Nowadays, the reinforced concrete, after more than 100 years of use, has shown its vulnerability to the action of time, weathering and earthquakes. The proportions and the typologies of the phenomena are such as to inhibit any solution merely based on classical restoration methods; therefore, in the recent years there is a growing interest in the knowledge of degradation processes, in the rehabilitation of reinforced concrete structures, and in the safeguard of the existing buildings in order to increase the coefficients of structural safety.

The production of cement and concrete is a highly energy-intensive process and contributes to the release of pollutants into the atmosphere due to both the chemical reactions occurring in the kiln and, in most cases, the burning of fossil fuels for power production. For example, in the USA, the average energy consumption for a cement plants is estimated to be about 5.1 GJ per metric ton of cement. Cement production also releases 0.98 tons of equivalent CO_2 per ton of cement clinker produced [1] with the total CO_2 eq. emission by the cement manufacturing industry in 2009 being an estimated 45.6 Tg (teragrams) CO_2 eq. Thus, the construction industry is identified as one

Published online: 26 April 2016

Table 1 Description of the mixtures and nanoparticles used: for each set

Sample description	Sample name	Diameter (nm)	Mix name	Mix set
Control samples (no fillers)	Control	–	Mix 1	A1–A9 (9 mortar)
Silica nanoparticles (SiO_2) non-porous	USA 20 NP	20	Mix 2	B1–B9 (9 mortar)
Silica nanoparticles (SiO_2)	USA 20–60	20–60	Mix 3	C1–C9 (9 mortar)
Silica nanoparticles (SiO_2)	USA 15–20	15–20	Mix 4	D1–D9 (9 mortar)
Hematite nanoparticles (α-Fe_2O_3)	USA Fe_2O_3 α	20–40	Mix 5	E1–E9 (9 mortar)
Maghemite nanoparticles (γ-Fe_2O_3)	USA Fe_2O_3 γ	20–40	Mix 6	F1–F9 (9 mortar)
Silica fume microparticles	Fly ash	20–40	Mix 7	G1–G9 (9 mortar)

The compressive strength, tensile strength, chemical durability, water permeability, and effect of changing the mixing techniques on compressive strength are tested for each mixture

of the major contributors to greenhouse gas emissions [2]. Concrete is the largest volume-manufactured product on earth, with current estimates of global concrete production being approximately around 10 billion m^3 per year. Globally, concrete production expects to continue to increase due to massive infrastructure developments throughout the world and due to the increasing world population. Cement is only one of the components used in concrete and the amount of cement in a concrete mixture can vary, typically ranging from 180 to 600 kg/m^3 for ordinary to high strength concrete [3]. Thus, high CO_2 emissions from the construction industry are in part due to the large demand for concrete.

If the cement clinker fraction in concrete mixtures could be reduced, there will be a high potential for decreasing CO_2 emissions into the atmosphere from the construction industry and enhance sustainability.

Several studies have been conducted recently to examine the effects of adding nanosilica to the cement mortar to examine its mechanical properties. A review of the literature indicates that adding nanosilica to concrete enhances its mechanical properties and durability [4]. However, it is important to conduct new studies using specific cements and aggregates with added nanoparticles in order to better understand the interaction between these components and the kinetics of the process. Also, there is little knowledge on durability and nanocement together with long-term properties. The aim of this work is to study the effect of adding various types of nanoparticles to the cement mortar on enhancing its mechanical properties and durability. Also, this study aims at providing a cement mortar with ultrahigh performance for use in some special applications. Moreover, in case of use of nanoparticles, a smaller quantity of cement binder inside the mortar indirectly causes relevant positive effects on the reduction of carbon dioxide emission in the atmosphere. For comparison, some concretes containing fly ash (silica microparticles) aggregates were also prepared in order to compare them with the nanoparticles ones.

2 Experimental

In order to achieve the objectives, 56 mortar mixtures have been designed and prepared, and they are summarized in Table 1. Hematite (α-Fe_2O_3), maghemite (γ-Fe_2O_3) and three types of silica nanoparticles with different sizes were used for the different mixtures. For comparison, a mixture with silica fume microparticles was also prepared. In any case, a cement CEM I 42.5 R according to UNI-EN 197/1 and a water/cement ratio of 0.4 was used. Several investigations have been performed in all the samples of all mix sets in order to control the final properties of the obtained concretes such as the compressive strength, tensile strength, chemical durability, water permeability, and effect of changing the mixing techniques on compressive strength. Crystal phase analyses were carried out by using X-ray diffraction (XRD) Bruker-AXS D5005, microstructure analysis using scanning electron microscopy (FED-SEM equipped with EDX) LEO Supra 55 VP, and surface studies, X-ray photoelectron spectroscopy (XPS), for studying the interactions of the nanoparticles with the alkaline medium by an instrument PHI ESCA/SAM 5600.

2.1 Synthesis of the nanoparticles

Nanoparticles of SiO_2 were prepared by sol–gel method. Stoeber et al. [5] first used this method for the production of nanosilica. In our work, we used a new method to produce this kind of nanoparticles using different evolution of sol–gel methods [6, 7] modified by us.

The silica particles were obtained by hydrolysis of tetraethyl orthosilicate (TEOS) (99.99 % Sigma-Aldrich) in ethanol medium (99.99 % Sigma-Aldrich) and water Millipore. Ammonia (28 % Sigma-Aldrich) was used as a catalyst. The reagents were used as prepared without any purification. Different reagents have effects on particle sizes. Using this method, it is possible to synthesize various-sized particles in the range 20–460 nm by varying concentration and temperature condition. The reagents used are ammonia (2.8–28 mol/L), ethanol (1–8 mol/L),

water (3–14 mol/L) and TEOS (0.012–0.12 mol/L), and particle size was examined under scanning electron microscopy (SEM) and dynamic light scattering (DLS).

The solutions were prepared in a glove box at room temperature under N_2 dry air.

A schematic design of a semibatch process is described in Fig. 1. The apparatus consists of a reservoir of starting solutions, a microfeed pump to supply the solutions, a water bath and a reactor with stirrer. A microfeed pump with a constant flow rate fed the starting solution (TEOS and ethanol) into the reactor that contains another solution (water, ethanol and ammonia), and the experiment was conducted with dry nitrogen.

Table 2 shows the correlation between reagents percent and temperature. The characterization of the average particle size was done with SEM and DLS.

Table 2 shows how the selected parameters ([H_2O]/[TEOS], concentration of ammonia, feed rate of reactant and reaction temperature) have effects on properties of the nanoparticles (particle size and size distribution).

For testing the mechanical properties of the SiO_2 nanoparticles as an additive in concrete, we chose the nanoparticles with this average size:

SiO_2 size: 20 nm non-porous;
SiO_2 size: 20–60 nm porous;
SiO_2 size: 15–20 nm porous.

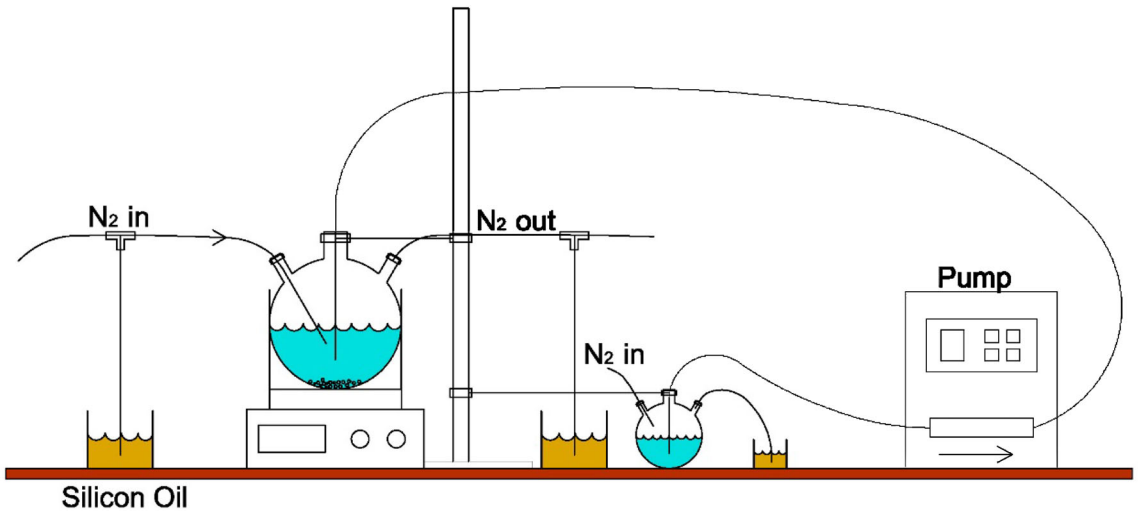

Fig. 1 Schematic design of the semibatch process for sol–gel synthesis

Table 2 Correlation between reagents percentage and temperature

Experiment	Conditions				Results	
	H_2O/TEOS	Feed rate (cm^3/min)	NH_3 (mol/l)	Temperature (°C)	Average particles size (nm)	Standard deviation (±nm)
1	25	0.6	0.2	15	71.2	8.4
2	25	18	1.0	15	65.5	6.8
3	25	0.6	1.0	70	35.5	7.2
4	25	18	0.2	70	11.2	3.1
5	90	9.3	0.6	42.5	120.7	8.4
6	90	9.3	0.6	42.5	129.4	8.0
7	90	9.3	0.6	42.5	125.3	7.1
8	90	9.3	0.6	42.5	118.7	7.3
9	155	0.6	1.0	15	245.8	10.4
10	155	18	0.2	15	132.4	8.1
11	155	0.6	0.2	70	33.5	4.2
12	155	18	1.0	70	148.5	9.6

In this work, we prepared two different types of Fe_2O_3 nanoparticles:

α Fe_2O_3 (hematite)
γ Fe_2O_3 (maghemite).

Nanoparticles of α Fe_2O_3 (hematite) were prepared by sol–gel method. We have prepared these particles by a Matijevic et al. [8] modified method for greater simplicity.

Two hundred milliliters (0.1 M) of iron nitrate $Fe(NO_3)_3 \cdot 9H_2O$ (Sigma-Aldrich 98 %) was used as a precursor solution and was gelified using 800 mL of monohydrated citric acid (Sigma-Aldrich 98 %) solution (0.05–0.2 M) as ligand molecules and distilled water as the solvent. The iron solution was added to the citric acid solution dropwise with vigorous stirring. The solution was then heated to a temperature of 70 °C, while maintaining vigorous stirring until the gel was formed and the contained water was evaporated. The dried gel was annealed at temperatures ranging from 180 to 400 °C, typically yielding Fe_2O_3 nanoparticles with size of 22–60 nm.

Nanocrystals of γ Fe_2O_3 (maghemite) were synthesized by emulsion precipitation method using kerosene as oil phase, SPAN-80 (sorbitan monooleate) as the surfactant and sodium hydroxide as the precipitating agent.

Anhydrous $FeCl_3$, NaOH, SPAN-80 (all of Analytical grade) and kerosene were used without further purification. Two hundred milliliters of $FeCl_3$ solution of 0.5 M was taken in a 1000 mL beaker. Two grams of SPAN-80 nonionic surfactant (sorbitan monooleate) was added with vigorous stirring, and the contents were stirred for 15 min. Four milliliters of kerosene was added, and stirring was continued for another 30 min. The system transformed to turbid emulsion of milky brown color. NaOH solution (5 M) was added dropwise till the pH reached up to 10–10.5. Reddish brown precipitate of iron hydroxide started forming from pH 3 onwards. Precipitate became thick as pH increased. After reaching the desired pH, addition of NaOH was stopped and the stirring continued for 1 h. The contents in the beaker were then left undisturbed for 30 min to allow the precipitate to settle. The precipitate was filtered and washed with distilled water till free of ions and excess alkali. Then, it was washed with acetone to remove kerosene and surfactant and was kept in an oven at 100 °C overnight. The dried precursor was subjected to calcination at various temperatures, i.e., 250, 500 and 850 °C for 2 h. After cooling and drying, final product was ground with agate mortar to get fine powder.

2.2 Preparations of the samples

In order to investigate the properties of nanoparticles of silica, hematite and maghemite, as well as fly ash microparticles, with specific reference to chemical interactions and interphase on surface between these and the cementitious binder, it was considered appropriate to establish an experimental set that reproduces the environment strongly basic of concrete paste.

We prepared some supports for the deposit of the nanoparticles on crystalline silicon, suitable as a stab of the instruments.

We fixed by direct contact the nanoparticles of different types of material on carbon strips. To eliminate the excesses of particles deposited on the surface of the specimens, we have placed the samples in a sonicator for 10 min at ambient temperature. All the samples were dried under continuous flow of dry nitrogen, into a glove box, under a hood in a controlled atmosphere to prevent contact with the carbon dioxide of the air. The samples were positioned, always in a controlled atmosphere, in cuvettes hermetically closed where a sufficient quantity of lime solution was introduced; the surface of the solution has been sprayed with dry nitrogen in order to avoid contact with the carbon dioxide present in the air and thus prevent the possibility that the calcium hydroxide $Ca(OH)_2$ binds, to form calcium carbonate ($CaCO_3$), on the surface. The samples remained in these conditions, for different periods of time (1, 24 h and 7 days). After the necessary time, a mild drying was carried out with nitrogen flow, and then, the samples were exposed to a more long and careful drying by placing them in an oven at a temperature of 31 °C for several hours. The operation was considered necessary in order to eliminate any trace of residual water which would have affected the subsequent steps.

Before each measurement, XPS samples were degassed in pre-chamber for at least 1 h in high vacuum conditions.

2.3 Characterization

XRD measurements of the samples of silica nanoparticles confirm the amorphous nature of these substances (very large peaks), as shown in Fig. 2.

Concerning the samples of nanoparticles of iron oxides, the diffractograms performed on two samples show the crystalline form of hematite (α Fe_2O_3) and maghemite (γ Fe_2O_3) (Fig. 3).

To determine the reactivity, the kinetics and the interaction between the nanoparticles of silica and lime, XPS measurements were taken on samples treated in alkaline solution, respectively, for 1, 24 h and 7 days. A quantitative analysis was carried out to assess the concentration of calcium present compared to that of silicon, in the various cases.

2.3.1 Silica nanoparticles, 1 h aged

The survey spectrum shows the presence of the following elements: carbon, oxygen and silicon, and calcium is almost nonexistent. The same goes for what concerns all the other samples aged for 1 h (Fig. 4).

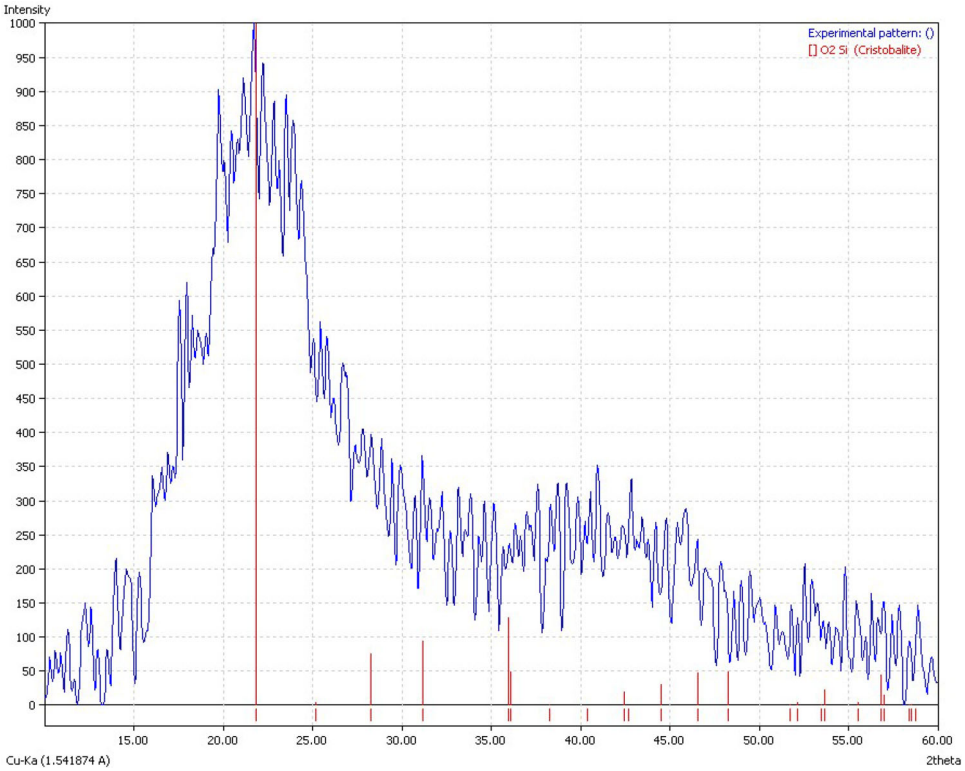

Fig. 2 XRD spectra of SiO_2 nanoparticles 40 nm

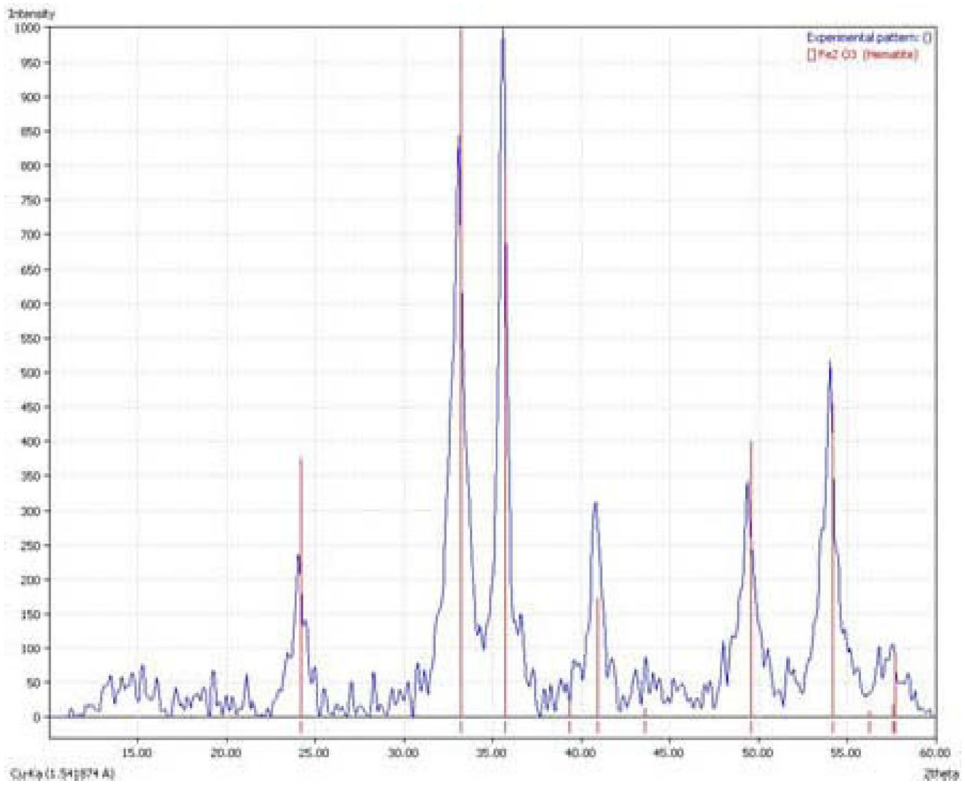

Fig. 3 XRD spectra of αFe_2O_3 hematite nanoparticles

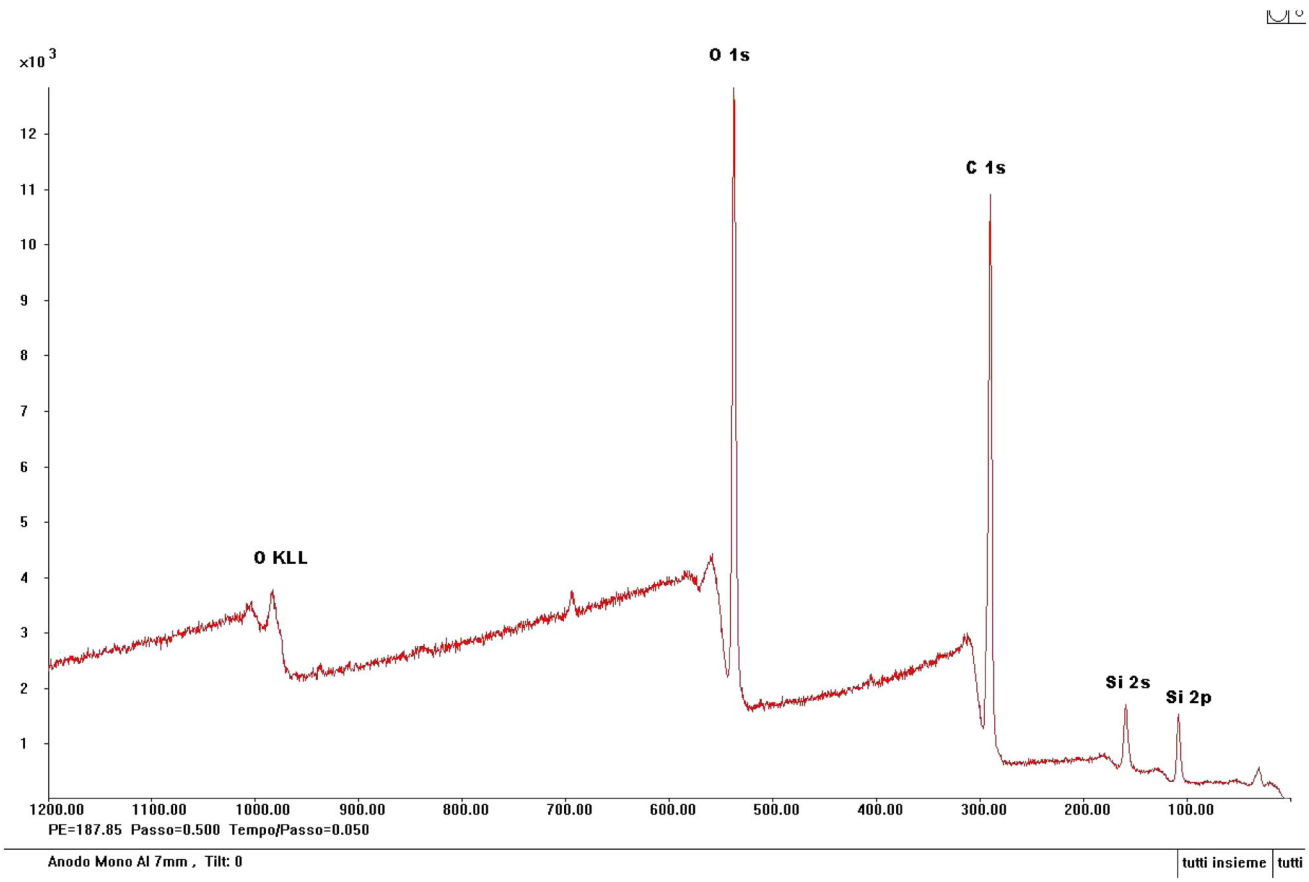

Fig. 4 Wide scan of silica nanoparticle aged 1 h

This result makes us assume that the 1-h reaction between silica nanoparticles and calcium hydroxide does not produce any significant effects at the nanoparticle surfaces. The multiplex spectra have confirmed this evidence.

2.3.2 Silica nanoparticles, 24 h aged

In addition to the signals related to the elements first traced, the expanded XPS spectra show the presence of calcium (Fig. 5).

The quantitative analysis performed for the evaluation of the concentration of calcium 2*p* and silicon 2*p* shows a significant, albeit modest, value of calcium bound on the surface of the sample. The relative atomic concentrations calculated after the fitting of the curves are:

Silicon 90.33 % – Calcium: 9.66 %.

2.3.3 Silica nanoparticles, 7 days aged

The XPS quantitative analysis reveals a lower calcium content compared to the previous case. Differences can be due both to little differences in the size of nanoparticles and to the intrinsic errors of the XPS measurements. The relative concentrations calculated after the fitting of the curves are:

Silicon 92.51 % – Calcium: 7.48 %.

Also in the case of hematite and maghemite nanoparticles, it is possible to see the presence of calcium after 24 h of aging (Fig. 6).

2.4 Physical tests

After the first phase of in-lab characterization, we moved to carry on some physical test in real scale.

For this purpose, it was taken into consideration the Lyse's Rule laying a quantity of water (kg/m^3) necessary to obtain the requested workability (Lm).

We used a type of cement according to UNI-EN 197/1: CEM I 42.5 R. The abbreviation R is to indicate a type of quick-setting cement.

As aggregates, we used two different rubbles of limestone with 20 and 10 mm of average diameters and a river sand with particle size distribution from 0.62 to 4.00 mm.

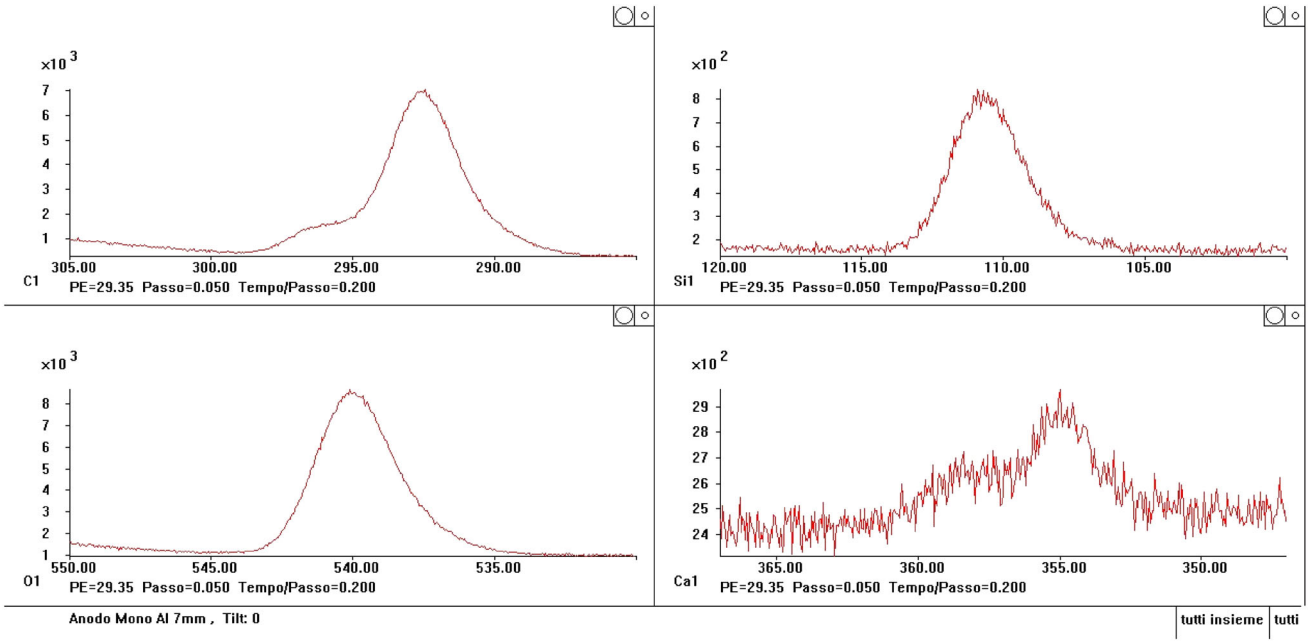

Fig. 5 Elements scan of silica nanoparticle aged 1 h

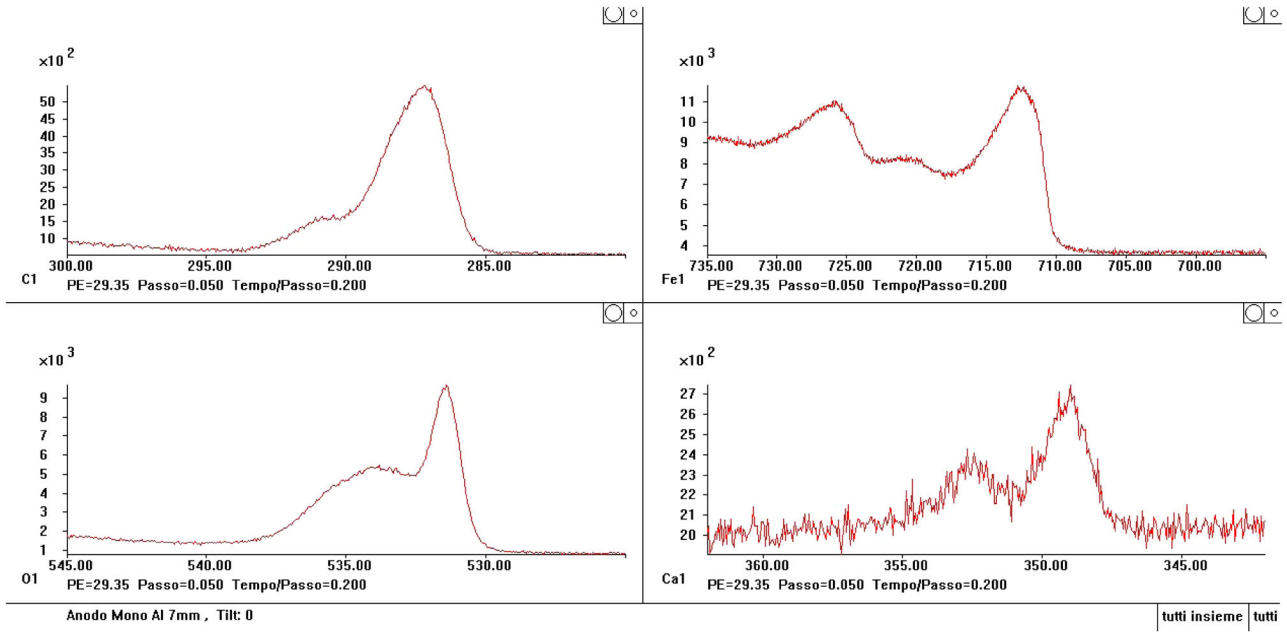

Fig. 6 Multi-element scan of hematite nanoparticle aged 24 h

Table 3 Mix design without nanopowders

Volume (m^3)	Rubble 1 (kg)	Rubble 2 (kg)	Sand (kg)	Cement (kg)	Water (l)	Additive (l)	Nano powers (kg)
0.0210	1.3	8.4	24.1	8.5	4.25	0.085	0

It was provided a quantity of water so that the ratio w/c was equal to 0:50. This quantity took into account the moisture of the aggregates, previously determined.

In order to allow adequate workability of the mixes, especially those containing the nanosilica fillers, we opted for the use of a super-plasticizer: AS

Table 4 Mix design with nanopowders

Volume (m^3)	Rubble 1 (kg)	Rubble 2 (kg)	Sand (kg)	Cement (kg)	Water (l)	Additive (l)	Nano powers (kg)
0.0150	1.0	6.0	17.2	5.858	3.050	0.061	0.242

SUPERFLUX of Axim (Italcementi Group), in the proportion of 1 %.

Ultimately, the following table summarizes the mix design (Table 3).

With this mixture were prepared seven cylindrical specimens with a diameter of 100 mm and height of 200 mm, and six cylindrical specimens with a diameter of 100 mm and height of 100 mm.

The water/cement ratio equal to 0.50 corresponded to a lowering of the Abrams cone (Slump) of 24 cm and then, from the point of view of rheological properties, to a workability S5 (Table 4).

With the mentioned amount of materials, four cylindrical specimens having a diameter of 100 mm and height of 200 mm and seven cylindrical specimens with a diameter of 100 mm and height of 100 mm were prepared. The addition of the nanoparticles to the concrete mix induced a drop of the Slump to 13 cm, compatible with workability S3.

In order to obtain maximum dispersion and homogenization of the nanoparticles in the dough, the dry components were mixed for few minutes; the amount of water and super-plasticizer provided were added and stirred to obtain the requested workability.

Compressive strength development of the concrete incorporating different types of nanoparticles of silica is given in Fig. 7b, in comparison with an ordinary Portland cement and with reference to a silica fume-doped concrete. The results show that the replacement with SiO_2 nanoparticles up to 4.0 % in wt produces high strength with respect to the reference concretes. Figure 7a shows the effect of nanoparticles of Fe_2O_3 on the compressive strength of the concrete compared to the reference ones. By comparing the compressive strength of specimens cured for 3, 7 and 28 days, it could be observed that the compressive strength increases when nanopowders particles are added, but the results show that it is smaller than the corresponding strength of silica fume series.

The permeability tests, carried out at low pressure on the specimens, show a higher resistance to water penetration (only 15 mm) of samples doped with silica nanoparticles compared to those with iron nanoparticles and to the reference sample (about 20 mm). The water permeability is an important parameter for the durability of a concrete because the cement protects the iron rebars of reinforced concrete structures.

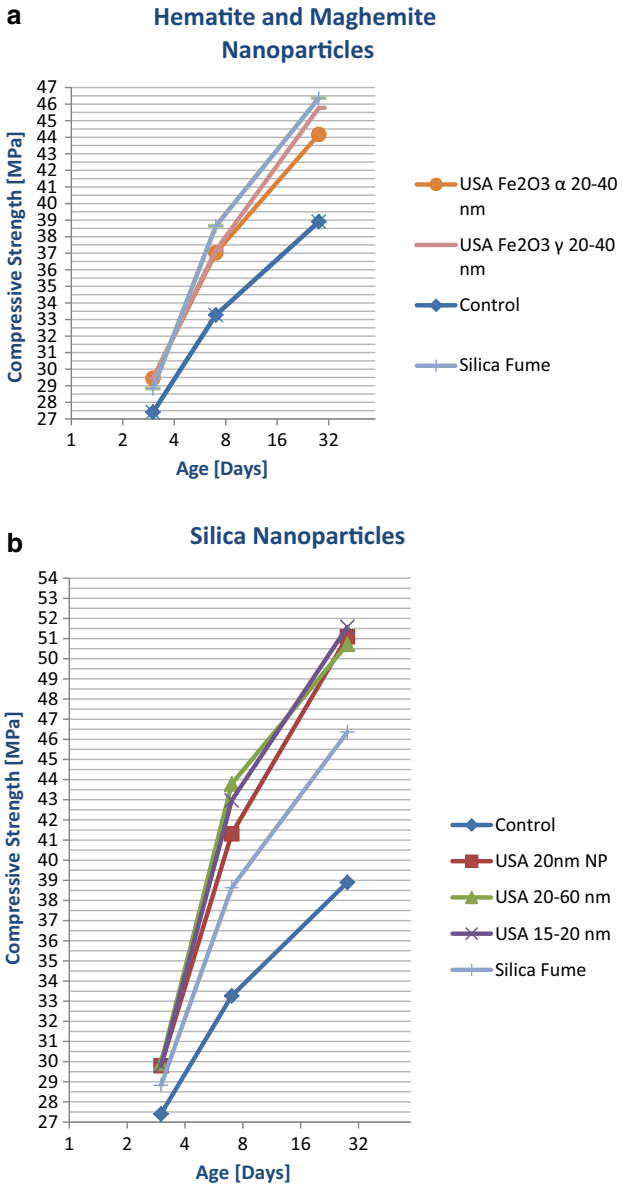

Fig. 7 **a** Compressive strength tests of hematite- and maghemite-doped concretes compared with normal concrete without nanoparticles. **b** Compressive strength tests of silica-doped concretes compared with normal concrete without nanoparticles

By experimental observations performed by ultrasonic tests, linear relations, which bind the values of dynamic elastic modulus of the various conglomerates to the respective resonant frequencies, have been obtained. The results of these tests are shown in the graph of Fig. 8.

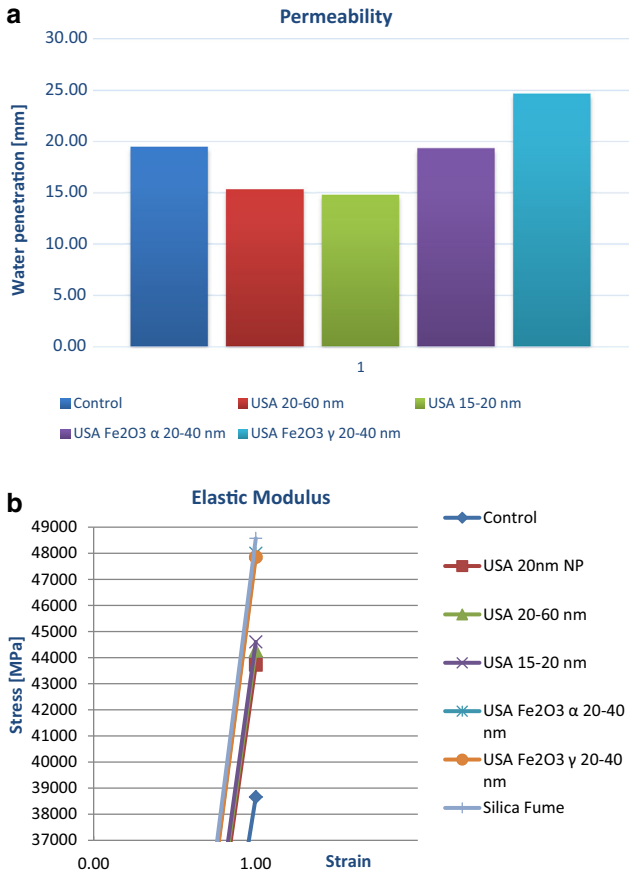

Fig. 8 Elastic modulus and permeability tests carried out on doped concretes compared with normal concrete without nanoparticles

3 Conclusion

The replacement of Portland cement with a small quantity (4 wt%) of silica nanoparticles and Fe_2O_3 nanoparticles yields a composite system showing higher performances in comparison with the common Portland concretes even with the addition of silica fume ashes. Compressive strength, water resistance and elastic modulus appear to have increased in these new composite materials. The pozzolanic reactions between the nanoparticles and the portlandite phase of the cement appear after 24 h and continue until the complete maturations of the concretes.

According to the obtained results, they can be a great candidate as innovative systems for the making of a new generation of contemporary buildings and structures or for the restoration of historical concrete architectures. In particular, the low water permeability enables the concrete to be more resistant to carbonation processes that are responsible for the iron oxidation in the reinforced concretes. We strongly recommend the use of these types of nanofillers because, as demonstrated by this work, obtaining the same mechanical performance (or better) we can achieve a reduction of CO_2 emissions in the production processes of 4 % (equal to the weight of Portland cement replaced in mix design). Using the data available in the literature [2], we can estimate a reduction of 1.8 Tg CO_2 eq. per year.

Other tests are currently being prepared and will include the use of full-scale structures such as beams and pillars in order to better study the interactions with urban environment.

Acknowledgments This research was supported by Regione Sicilia Grant POR-FESR Sicilia 2007/2013, line 4.1.1.2. CUP: G53F11000080004.

References

1. A. Kapur et al., The contemporary cement cycle of the United States. J. Mater. Cycles Waste Manag. **11**(2), 155–165 (2009)
2. L. Vukotic, R.A. Fenner, K. Symons, Assessing embodied energy of building structural elements. Proc. Inst. Civil Eng. Eng. Sustain. **163**(3), 147–158 (2010)
3. P.K. Mehta, P.J.M. Monteiro, *Concrete—Microstructure, Properties and Materials* (McGraw-Hill, New York, 2006)
4. V.V. Vikulin, M.K. Alekseev, I.L. Shkarupa, Study of the effect of some commercially available nanopowders on the strength of concrete based on alumina cement. Refract. Ind. Ceram **52**, 288–290 (2011)
5. W. Stober, A. Fink, Controlled growth of monodisperse silica spheres in the micron size range. J. Colloid Interface Sci. **26**(1968), 62–69 (1967)
6. S.K. Park, K.D. Kim, H.T. Kim, Preparation of silica nanoparticles: determination of the optimal synthesis conditions for small and uniform particles. Colloids Surf. A **197**(2002), 7–17 (2001)
7. K.S. Rao, K. El-Hami, T. Kodaki, K. Matsushige, K. Makino, A novel method for synthesis of silica nanoparticles. J. Colloid Interface Sci. **289**(2005), 125–131 (2005)
8. E. Matijević, P. Scheiner, Ferric hydrous oxide sols: III. Preparation of uniform particles by hydrolysis of Fe(III)-chloride,-nitrate, and-perchlorate solutions. J. Colloid Interface Sci. **63**(3), 509–524 (1978)